Ruhr-Universität Bochum
Lehrstuhl für Automatisierungstechnik
und Prozessinformatik

Forschungsbericht

J. Lunze, P. Planchon, M. Rode, M. Schneider

A cold rolling mill model for unwinding diagnosis

submitted for4th MATHMOD Conference

Januar 2003 Bericht Nr. 2003.1

A COLD ROLLING MILL MODEL FOR UNWINDING DIAGNOSIS

P. Planchon and J. Lunze, Ruhr-Universität Bochum, Germany
M. Rode and M. Schneider, Asea Brown Boveri (ABB), Germany

Corresponding author: P. Planchon
Lehrstuhl für Automatisierungstechnik und Prozessinformatik
Ruhr-Universität Bochum
44780 Bochum, Germany
Phone: +49 234-32-26632, Fax:+49 234-32-14101
Email: planchon@atp.ruhr-uni-bochum.de

Abstract. A model is presented which describes the uncoiling process of a rolling mill in fault-less and in faulty situations. This model is implemented in the DYMOLA modelling and simulation environment. It is used for two purposes: first for the *simulation* of the unwinding process and second for *model-based fault diagnosis*. For the latter diagnostic task, a simplified model is derived. Results of the successful diagnosis, in simulation, concludes the paper.

1 Introduction – Motivation

Developing process supervision tools for complex or automated systems is becoming increasingly important. This is not only motivated by higher security standards but also because unplanned down-times of a factory or reduced quality of the end-product lead to considerable costs.
Although some supervision can already be achieved without using very precise knowledge about the process by, for example, signal trend analysis, model-based supervision methods allow to deal with more subtile situations, *e.g.* when faults modify the dynamics of the system only. This type of method requires adequate process knowledge, such as a mathematical model, to achieve the diagnosis.

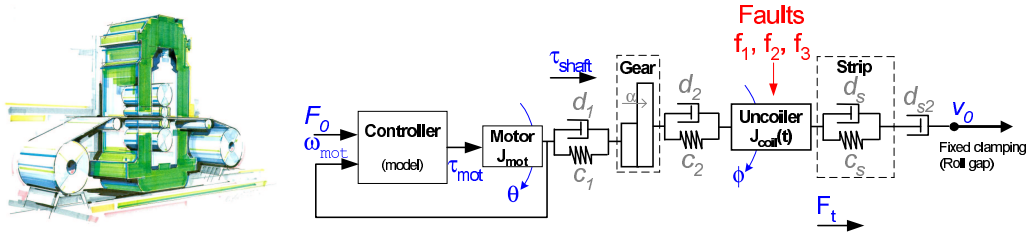

(a) Single stand mill, from left to right: uncoiler, stand and coiler.

(b) Physical chain of components considered in the unwinding process: controller, motor, shafts, gear, uncoiler and strip.

Figure 1: System under consideration

The focus of this paper lies on the modelling of the *uncoiler process* of a rolling mill. In this process a metal strip is unwinded into a single stand cold rolling mill (Figure 1(a)) where its flatness or thickness is corrected to reach a desired level. The proposed modelling is pursued in order to study the *diagnosability* of such systems, *i.e.* the possibility to detect the presence of faults during the operation of the system. Section 2 presents the detailed model of the uncoiling process. This fault-free *process model* is then extended in Section 3 to include possible faulty behaviours. The simplification proposed in Section 4 yields a *diagnostic model* that can be used for fault detection as illustrated in Section 5. Using both the process and the diagnostic models, results of the fault detection in simulation are presented.

2 Uncoiler process model

2.1 Modelling assumptions

This section presents the model used for simulating the uncoiler in fault-free operation. As seen from Figure 1(b), the "uncoiler process" under consideration is not limited to the physical uncoiler component but expands from the drive control to the roll gap.
The process has two inputs, the set-point F_0 of the motor controller and the mill speed v_0 which is fixed by the stand. The strip is winded with an initial radius R_0 and has specific metal properties (stiffness, hardness, thickness h_0, width W, *etc.*). The process has to be modelled using both a motor angle (θ) and a coiler angle (ϕ). These angles defer in amplitude because of the gear, but also in their dynamics because of the non-rigid shafts connecting them together.

Since the process model is seeked to demonstrate the diagnosability of the unwinding process, the study restrains itself to specific working conditions. A "fixed clamping" is imposed at the roll gap, *i.e.* the strip speed v_0 through the mill is supposed to be constant. Hence, the acceleration and deceleration phases are not considered. Moreover the plastic deformation occurring in the roll gap is neglected.
The uncoiler model is implemented using the *Dymola* modelling tool [6]. In-depth details on the mechanics of rolling mills can be found in [1, 3].

2.2 Components equations

Motor. The electric transfer function in the motor from input signal (issued by the controller) to the mechanical torque τ_{mot} is neglected since its dynamics are a lot faster than that of the unwinding process. Because of this, Figure 1(b) shows τ_{mot} as an output signal of the controller.
Therefore, the motor is modelled with a fixed inertia J_{mot} driven by a torque τ_{mot} "from the controller" and transmitting τ_{shaft} further on. The equation below shows how the generated torque τ_{mot} is transformed into both a rotation of the motor ($\ddot{\theta}$) and a transmitted torque τ_{shaft} to the shaft:

$$\tau_{mot}(t) = J_{mot}\,\ddot{\theta} + \tau_{shaft}(t) \quad . \tag{1}$$

Gear and shaft. The torque τ_{shaft} can be computed from the spring-damping coefficients $\{c_1,c_2,d_1,d_2\}$ and the gear ratio $\{\alpha\}$. Since the elements characterised by the parameters $\{c_1,d_1\}$ and $\{c_2,d_2\}$ are located on different side of the gear, a slight transformation has to be done leading to:

$$\begin{aligned} \tau_{shaft} &= \gamma_c\,(\theta - \alpha\phi) + \gamma_d\,(\dot{\theta} - \alpha\dot{\phi}) \\ \text{with} \quad \gamma_c &= \frac{c_1 c_2}{\alpha^2 c_1 + c_2} \text{ (equivalent spring)} \\ \text{and} \quad \gamma_d &= \frac{d_1 d_2}{\alpha^2 d_1 + d_2} \text{ (equivalent damper).} \end{aligned} \tag{2}$$

Coiler. The uncoiler system has a *time-varying* inertia, since its size (radius R_{coil} and moment of inertia J_{coil}) diminish with increasing time.
The two torques τ_{shaft} and τ_{strip} act on its rotation. τ_{shaft} represents the portion of the motor's torque that is transmitted through the gear. τ_{strip} is the torque generated as the metal strip is pulled into the roll gap and depends on the current strip tension F_t and coiler radius R_{coil}.

$$\begin{aligned} \frac{\mathrm{d}(J_{coil}\,\dot{\phi})}{\mathrm{d}t} &= \alpha\,\tau_{shaft} + \tau_{strip} \\ \frac{\mathrm{d}J_{coil}}{\mathrm{d}t}\,\dot{\phi} + J_{coil}\,\ddot{\phi} &= \alpha\,\Big(\gamma_c\,(\theta - \alpha\phi) + \gamma_d\,(\dot{\theta} - \alpha\dot{\phi})\Big) + F_t\,R_{coil} \quad . \end{aligned} \tag{3}$$

J_{coil} and R_{coil} can be integrated from $\dot{\phi}$ using

$$\dot{R}_{coil} = -\frac{h_0}{2\pi}\,\dot{\phi}, \qquad \dot{J}_{coil} = -\rho\,W\,h_0\,R_{coil}^3\,\dot{\phi}, \tag{4}$$

where ρ, W and h_0 are the strip density, width and thickness.

PSfrag replacements

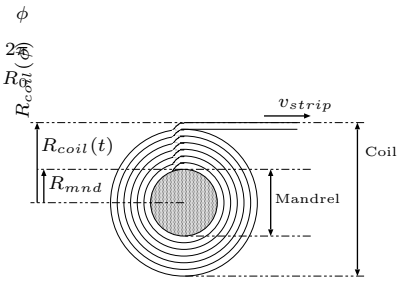

Figure 2: Section of an uncoiler winding

Controller. The controller computes a model-adaptive torque τ_{mot} the motor must generate for a given set-point F_0 and the measured rotating speed $\omega_{mot} = \dot{\theta}$. Reformulating Equations (1) and (3) using simplifications one obtains

$$\tau_{mot} = \frac{1}{\alpha}\left(-F_0\, R_{ctrl} + \left(\dot{J}_{ctrl} - J_{ctrl}\frac{\dot{R}_{ctrl}}{R_{ctrl}}\right)\frac{\dot{\theta}}{\alpha}\right), \tag{5}$$

where R_{ctrl} and J_{ctrl} are the approximations of the current radius and inertia as computed in the controller by integrating Equations (4) online. Noticeably the feedback loop for this controller only uses information of the motor revolution ω_{mot}, although the strip tension F_t is considered a measurement during the diagnosis (see Section 5). Reason for this is that F_t is not a standard measurement found on all mills and is therefore not used in the controller design.

Strip. The conversion from a rotational to a translational movement occurs at the uncoiler exit. The spring is modelled as a spring-damper system. Between the uncoiler and the mill stand (roll gap), the elongation of the strip Δ_l and the speed difference Δ_v can be computed from $\Delta_v = v_0 - R_{coil}\,\dot{\phi}$ and $\Delta_l = \int \Delta_v$. Considering only the two parallel components c_s and d_s (see Figure 1(b)), the strip tension F_t is computed as

$$F_t = d_s\,\Delta_v + c_s\,\Delta_l \quad . \tag{6}$$

2.3 Overall nonlinear model of the uncoiler

Using the state vector $X = [\theta, \dot{\theta}, \phi, \dot{\phi}, R_{coil}, J_{coil}, \Delta_l]^T$, Equations (1)–(6) can be summarised into nonlinear state space description

$$\begin{aligned}
\dot{\theta} &= \frac{\mathrm{d}\theta}{\mathrm{d}t}\\
\ddot{\theta} &= \frac{1}{J_{mot}}\,\tau_{mot} + \frac{\gamma_c}{J_{mot}}(\alpha\,\phi - \theta) + \frac{\gamma_d}{J_{mot}}(\alpha\,\dot{\phi} - \dot{\theta})\\
\dot{\phi} &= \frac{\mathrm{d}\phi}{\mathrm{d}t}\\
\ddot{\phi} &= -\frac{\dot{J}_{coil}}{J_{coil}}\,\dot{\phi} + \frac{1}{J_{coil}}\,F_t\,R_{coil} - \frac{\alpha\,\gamma_c}{J_{coil}}(\alpha\,\phi - \theta) - \frac{\alpha\gamma_d}{J_{coil}}(\alpha\,\dot{\phi} - \dot{\theta})\\
\dot{R}_{coil} &= -\frac{h_0}{2\pi}\,\dot{\phi}\\
\dot{J}_{coil} &= -\rho\,W\,h_0\,R_{coil}^3\,\dot{\phi}\\
\dot{\Delta}_l &= v_0 - R_{coil}\,\dot{\phi}
\end{aligned}$$

with

$$\begin{aligned}
F_t &= c_s\,\Delta_l + d_s\dot{\Delta}_l = c_s\,\Delta_l + d_s\,(v_0 - R_{coil}\dot{\phi})\\
\tau_{mot} &= \frac{1}{\alpha}\left(-F_0\,R_{ctrl} + \frac{\dot{\theta}}{\alpha}\left(\dot{J}_{ctrl} - \frac{\dot{R}_{ctrl}}{R_{ctrl}}J_{ctrl}\right)\right) \quad .
\end{aligned}$$

The controller parameters are derived from the expected unwrapping behaviour of Equations (4), but using the available measurement $\dot{\theta}$, such that

$$\dot{R}_{ctrl} = -\frac{h_0}{2\pi}\left(\frac{\dot{\theta}}{\alpha}\right), \qquad \dot{J}_{ctrl} = -\rho\, W\, h_0\, R_{ctrl}^3 \left(\frac{\dot{\theta}}{\alpha}\right).$$

As mentioned in the beginning of this section, the process model is considered at constant roll gap speed v_0. This implies an initialisation of the model starting at non-zero speed: (R_{mnd} and J_{mnd} are physical parameters of the mandrel)

$$\begin{aligned}
R_{coil}(t{=}0) &= R_0,\\
J_{coil}(t{=}0) &= J_0 = \rho\, W\, \frac{\pi}{2}(R_0^4 - R_{mnd}^4) + J_{mnd},\\
\dot{\theta}(t{=}0) &= \frac{V_0}{R_0}\alpha,\\
\dot{\phi}(t{=}0) &= \frac{V_0}{R_0},\\
\gamma_c\Big(\theta(t{=}0) - \alpha\phi(t{=}0)\Big) &= \tau_{shaft}(t{=}0) = \tau_{mot}(t{=}0),\\
\Delta_l(t{=}0) &= \frac{F_t(t{=}0)}{c_s} = \frac{F_0}{c_s}.
\end{aligned}$$

3 Extension of the system to fault cases

The model presented so far does not include possible fault effects. For diagnostic purposes it has to be extended to reproduce the faults which are to be detected. This section describes three faults under consideration and their integration in the *Dymola* model. The mathematical equations for each faulty system are not given, since only the fault-free model is necessary for fault detection.

3.1 Description of possible fault cases

Fault f_1: "mandrel slip." A slip occurs between the mandrel and the coil. This can occur as a result of a loose connection between the first layers of the strip and the mandrel. In the fault-free case, the mandrel and the coil rotate with a unified angle ϕ. In fault case f_1, the slip provokes a physical separation of the mandrel and the coil for a very short time. This requires to distinguish the two angles ϕ_1 (mandrel's rotation) and ϕ_2 (uncoiler's rotation). Therefore, the structure of the system is modified by the fault (increased system order).

Fault f_2: "coil slip." A slip occurs within the coil, between two strip layers. This is a very similar case to fault f_1 but with a stronger elasticity which needs to be taken into account. As for fault f_1, modelling the slip in case f_2 requires to split the angle ϕ into two angles ϕ_2 and ϕ_3. In fault case f_2, these angles represent respectively the rotation angles for the elements {mandrel+beginning of coil} and {end of coil}. The beginning of the coil refers to the deepest layers of the metal strip.

Fault f_3: "strip stick." In the fault-free case, the upper layer from the uncoiler regularly flows out into the roll gap. In fault case f_3, this upper strip layer suddenly "sticks" to the coil. This sticking provokes a sudden increase in the strip tension F_t. The longer the fault lasts, the higher is the increase. The fault strength increases with the rotation ϕ. When F_t reaches a critical level, the strip is freed suddenly, causing violent oscillations.

3.2 Extending the Dymola fault-free model to include the faults

This section shows how the considered faults are implemented in the object-oriented modelling tool *Dymola*. The global structure of the entire model is seen in Figure 1(b). Since all faults occur within the "uncoiler" block, only the Dymola model of this block is modified to include the fault components. Figure 4(a) shows the representation of the fault-free uncoiler. It is composed of three inertias for the mandrel, the inside of the winding (`Coil_inner`) and the time-varying inertia modelling the end (outside)

of the coil being unwinded (`Coil_outer`). The other blocks in the model assure the integration with the objects of higher order in the hierarchy of the overall process model.

To extend this model to the fault cases, additional interfaces have to be inserted at the precise location of the faults occurrences. The "clutch" and "brake" blocks from the Modelica Standard Library (Figure 3) are used to model the sliping and sticking effects which characterise the fault.

PSfrag replacements

PSfrag replacements

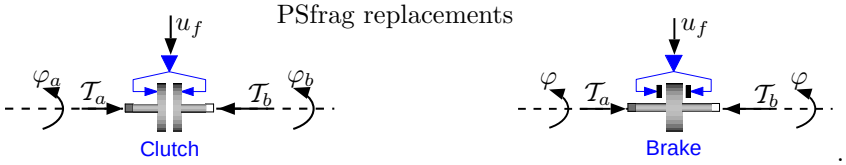

Figure 3: Standard Dymola blocks used in the fault modelling.

Behaviour of clutch block. The input u_f to the clutch determines the pressure force with which the clutch is maintained closed (*i.e.* $u_f = 0 \Leftrightarrow$ open clutch). The main clutch parameter is the torque $\mathcal{T}_{max}$ which scales the input. Let $\mathcal{T}_A$ and $\mathcal{T}_B$ be the incoming torques on each side of the clutch, and φ_a and φ_b the corresponding rotation angles. The model uses a so-called path parameter s to insure a smooth transition from the closed state (locked) into the open state (free). The clutch behaviour can be approximated as

$$\text{(free: faulty)} \qquad u_f \leq 0 \qquad \begin{cases} \mathcal{T}_A = -\mathcal{T}_B = 0 \\ \frac{\mathrm{d}^2}{\mathrm{d}t^2}(\varphi_b - \varphi_a) = s \end{cases}$$

$$\text{(locked: no fault)} \qquad u_f \cdot \mathcal{T}_{max} > \mathcal{T}_B \qquad \begin{cases} \mathcal{T}_A = -\mathcal{T}_B = s \\ \frac{\mathrm{d}^2}{\mathrm{d}t^2}(\varphi_b - \varphi_a) = 0 \end{cases}$$

The fault-free behaviour is associated with a locked clutch, whereas the faults f_1 and f_2 are simulated by opening the clutch for a brief time. To comply with the usual convention ($f = 0 \Leftrightarrow$ no fault), the implementation uses an "inverter" function such that $u_{f_1} = (1 - f_1)$ and $u_{f_2} = (1 - f_2)$, hence $f_i = 0$ implies fault-free behaviour as long as $\mathcal{T}_{max}$ is chosen big enough.

Behaviour of brake block. The input to the brake determines the brake force to apply to the rotating shaft. As opposed to the clutch, no physical separation occurs between each side of the brake block. The main parameter for the brake is the normalising torque $\mathcal{T}'_{max}$. Let $\mathcal{T}_A$ and $\mathcal{T}_B$ be the incoming torques on each side of the brake, and φ its rotation angle. The model uses a path parameter s, just as with the clutch. For fault case f_3, the blockage of the brake is not desired (equivalent to the "locked" state of the clutch), in practise this is avoided by insuring that the brake force ($u_f \cdot \mathcal{T}'_{max}$) never exceeds the shaft torque $\mathcal{T}_B$. The brake behaviour can be approximated as

$$\text{(free: no fault)} \qquad u_f \leq 0 \qquad \begin{cases} \mathcal{T}_A + \mathcal{T}_B = 0 \\ \frac{\mathrm{d}^2}{\mathrm{d}t^2}(\varphi) = s \end{cases}$$

$$\text{(braking: faulty)} \qquad u_f > 0 \qquad \begin{cases} \mathcal{T}_A + \mathcal{T}_B = \tau & \text{with } \tau = \mu_0 \, (u_f \cdot \mathcal{T}'_{max}) \\ \frac{\mathrm{d}^2}{\mathrm{d}t^2}(\varphi) = s - c\,\tau & \text{and } c \text{ a geometry constant.} \end{cases}$$

The brake already behaves following the convention ($u_f = 0 \Leftrightarrow$ no fault) so that $u_f = f_3$.

Figure 4(b) shows how the faults are implemented in Dymola. The model can simulate faulty behaviours when the fault signals f_i are non-zero. Using the Dymola object-oriented modelling, one sees immediately at which physical location the faults affect the system.

4 Simplified uncoiler model

In this section a simplification of the unwinding model from Section 2 is given. The simplifications are only seeked in the controller, motor and uncoiler components. The strip itself is not modelled (state

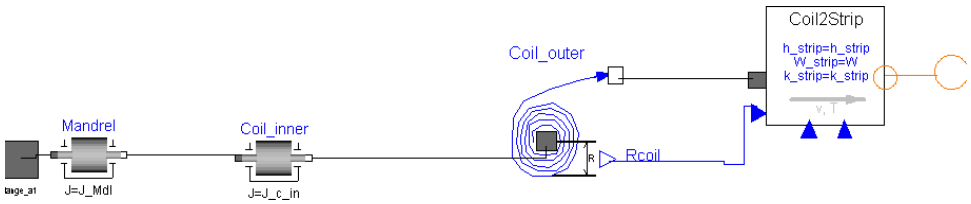

(a) Fault-Free model.

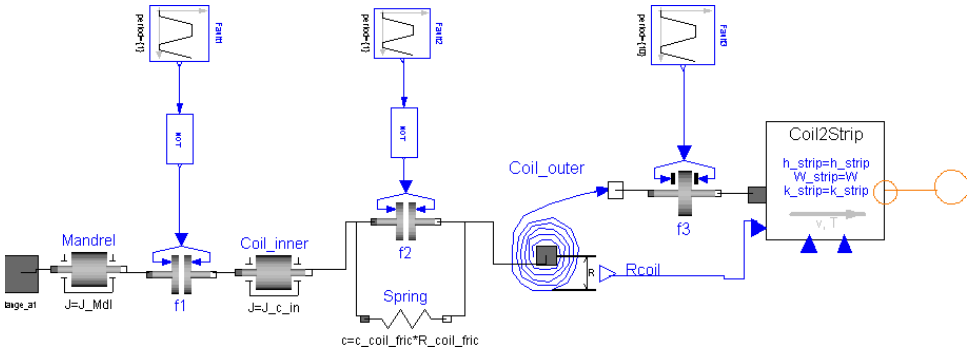

(b) Fault capable model.

Figure 4: Object decomposition of the "uncoiler" block from Figure 1(b), as found in Dymola.

Δ_l) since the strip tension F_t is directly measurable and will therefore not be needed for the diagnostic model. The proposed simplifications yield a fourth order linear model, which will be used for diagnosing the process in Section 5.

4.1 Assumptions used for the simplification

Because the faults under consideration strongly influence the system, but only for a short period of time, the model used for the diagnosis need only be valid for a limited time interval. Since the occurrence of faults provokes extremely fast dynamics in the process, the detection can succeed when using such a simplified model.
As a result of which, the main simplification proposed is to **fix the time-varying variables $\mathbf{R_{coil}}$ and $\mathbf{J_{coil}}$** by assuming their dynamic a lot slower then that of other states. This assumption reduces the order of the system and removes most of the nonlinearities found in the original process model.
The obtained uncoiling model still realistically describes the system but only for a limited time interval, typically a few seconds. This simplified model has a time-limited validity interval, *e.g.* $t = t_0 \ldots t_0 + T_{max}$. The duration of this validity interval depends mostly on the mill speed v_0.
The time-varying parameters of the uncoiler are fixed according to the following equations, in which t_0 represents the time at which the time-window begins:

$$
\begin{aligned}
R_{coil}(t) &\approx R_{coil}(t_0) = R_0 \\
\dot{R}_{coil}(t) &\approx \dot{R}_{coil}(t_0) = \frac{-h_0}{2\pi}\dot{\phi}(t_0) = \frac{-h_0}{2\pi}\frac{v_0}{R_0} \\
J_{coil}(t) &\approx J_{coil}(t_0) = J_0 = \rho\, W\, \frac{\pi}{2}(R_0^4 - R_{mnd}^4) + J_{mnd} \\
\dot{J}_{coil}(t) &\approx \dot{J}_{coil}(t_0) = -\rho\, W\, h_0\, R_0^3\, \dot{\phi}(t_0) = -\rho\, W\, h_0\, R_0^2\, v_0.
\end{aligned}
$$

These simplifications break the dynamic relationship between J_{coil} and $\dot{J}_{coil}$ since J_{coil} is set constant and $\dot{J}_{coil}$ is a non-vanishing constant. This is nevertheless justified by the need to preserve the order of

magnitude of certain parameters with respect to others. The obtained model is for use within a given time-window.

By **neglecting the closed-loop $\dot{\theta}$-terms in the controller** (see Equation (5)) further simplification is achieved. The resulting controller is open-loop:

$$\tau_{mot} \approx -\frac{F_0\, R_0}{\alpha}.$$

4.2 Equations of the simplified model

Rewriting the nonlinear model from Section 2.3 using the above simplification assumptions, lead to the following 4^{th}-order linear system in $(\theta, \dot{\theta}, \phi, \dot{\phi})$:

$$J_{mot}\,\ddot{\theta} = \frac{-F_0\, R_0}{\alpha} + \gamma_c(\alpha\phi - \theta) + \gamma_d(\alpha\dot{\phi} - \dot{\theta}) \tag{7}$$

$$J_{coil}(t_0)\,\ddot{\phi} = -\dot{J}_{coil}(t_0)\,\dot{\phi} + F_t\, R_0 - \alpha\,\gamma_c(\alpha\phi - \theta) - \alpha\gamma_d(\alpha\dot{\phi} - \dot{\theta}) \quad . \tag{8}$$

The tension set-point F_0 is an input to the model. As will be seen in the next section, the strip tension F_t will also be seen as an "input" to the diagnosis function, since it is considered to be measured. Figure 5 shows the block diagram representation of this system consisting of two 2^{nd} order subsystems for the motor and the uncoiler. Having input-output information for each of these blocks, it is conceivable to test the diagnosis methods as shown in the following section.

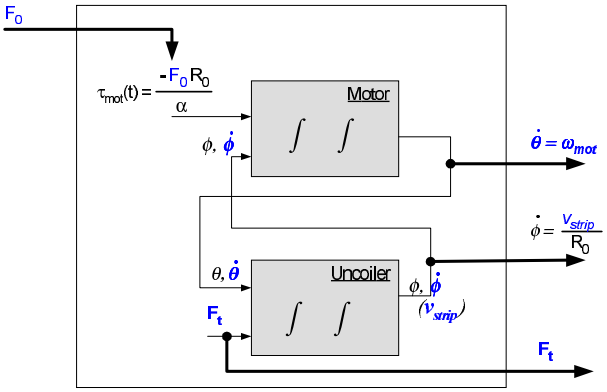

Figure 5: Block diagram of the simplified uncoiler model used for supervision. Process information (F_0, F_t, $\dot{\theta}$ and $\dot{\phi} \approx \frac{v_{strip}}{R_{coil}}$) are indicated by the signals coming in and out of the block. The details of the two second order models of the motor and the uncoiler are not shown for more clarity.

5 Model-based diagnosis of the uncoiler

This section briefly describes a model-based diagnostic method constructed using the models described in this paper. For further interest in the field of process supervision and model-based diagnosis, refer to [2, 4, 5].

Because faults cannot be intentionally provoked in an operating rolling mill and because process measurements corresponding to specific faults cannot be easily obtained, the nonlinear uncoiler process model derived in Section 2 is used as an input-output signal generator to test the effectiveness of diagnostic methods. The signals can be generated for specific operating conditions (set point for strip tension F_0, constant strip speed v_0, uncoiler's initial radius R_0, strip thickness h_0, occurrence and strength of a fault f_i).

5.1 Generating residuals

Using parity-space transformation, the simplified model from Section 4 can be reformulated to obtain *residuals* that indicate the presence of a fault. Under ideal conditions, a residual $r(t)$ is nonzero in faulty situations and vanish in fault-free operation. This behaviour cannot be met as such in practise, hence the use of a threshold δ in the evaluation of $r(t)$, such that an alarm is generated only when $\|r(t)\| > \delta$.

By moving each side of the two Equations (7) and (8) on a single side of the equality-sign,

$$R_1(t) := -J_{mot}\,\ddot{\theta} - \frac{F_0\,R_0}{\alpha} + \gamma_c(\alpha\phi - \theta) + \gamma_d(\alpha\dot{\phi} - \dot{\theta}) \tag{9}$$

$$\text{and } R_2(t) := J_{coil}(t_0)\,\ddot{\phi} + \dot{J}_{coil}(t_0)\,\dot{\phi} - F_t\,R_0 + \alpha\,\gamma_c(\alpha\phi - \theta) + \alpha\gamma_d(\alpha\dot{\phi} - \theta) \tag{10}$$

are obtained. The residuals (9), (10) measure the error resulting in the injection of the process measurements ($\dot{\theta}$, F_t, F_0, $\dot{\phi} \approx \frac{v_{strip}}{R_{coil}}$) into its expected mathematical representation (7), (8). Therefore, R_1 and R_2 are nonzero if, either a fault occurs (process does not behave according to model) or the model loses its validity. Faults can be successfully detected if they modify the system behaviour strongly enough to bring $R_1(t)$ or $R_2(t)$ over a preset threshold, and quickly enough so that the detection occurs within the validity time interval of the simplified model.

The residuals $R_1(t)$ and $R_2(t)$ must be computed using available process measurements only. As seen in Figure 5, these are ω_{mot}, F_t, F_0 and v_{strip}, from which the following variables are set

$$\dot{\theta} = \omega_{mot}, \qquad F_t = F_t, \qquad F_0 = F_0,$$

$$\dot{\phi} = \frac{v_{strip}}{R_{coil}} = \frac{v_{strip}}{R_0 - k\,(t - t_0)}, \quad \text{with } k = -\left.\frac{\mathrm{d}R_{coil}}{\mathrm{d}t}\right|_{t_0} = -\dot{R}_{coil}(t_0) = \frac{h_0}{2\pi}\frac{v_0}{R_0}$$

To generate completely the residuals, the following variables still have to be approximated:

$$\ddot{\theta} = \frac{\mathrm{d}}{\mathrm{d}t}\,\dot{\theta}, \qquad \theta = \int_{t_0}^{t} \dot{\theta}\,\mathrm{d}t + \theta_{ini}$$

$$\ddot{\phi} = \frac{\mathrm{d}}{\mathrm{d}t}\,\dot{\phi}, \qquad \phi = \int_{t_0}^{t} \dot{\phi}\,\mathrm{d}t + \phi_{ini}$$

In order to use the differentiation operator $\frac{\mathrm{d}}{\mathrm{d}t}(\cdot)$, it is considered ideal signals (noise-free). This can be assumed in a first step, since the aim of this study is to show whether *some* diagnosis may be successful, at least in ideal conditions.
The computation of $\dot{\phi}$ uses a time-varying radius. Without this adjustment, the measurement v_{strip} alone, only poorly represents the state $\dot{\phi}$. This remains consistent with the simplifications proposed in Section 4.1, since solely the information about the derivative $\dot{R}_{coil}(t_0)$ at the beginning of the time window is used.

5.2 Diagnostic results

The overall supervision system constructed using residual-based diagnosis is seen in Figure 6. In this section the *diagnosability* of the system should be analysed using the measurements obtained from the Dymola simulator in different operating modes (fault-free, and the 3 different fault cases) and using different input signals scenarios. The measurements obtained from simulation of the model in Section 2 are checked for consistency against the residuals computed in Section 5.1.

As an illustrative example, Figure 7 shows the residuals obtained for simulations in fault-free and fault case f_3. In the fault-free case (2 upper plots), the residuals grow exponentially, which is an expected consequence of the model simplification, which validity depreciates with time. As the coil is unwrapped, the values fixed in Section 4.1 for the radius R_{coil} and the inertia J_{coil} become increasingly wrong. Practically speaking, this requires reinitialising the simplified model after a given time window length.

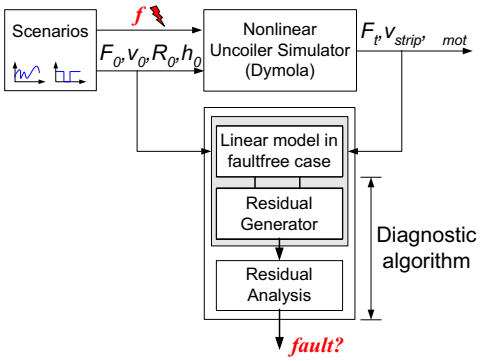

Figure 6: Structure of the tested model-based diagnosis method

By setting appropriate thresholds δ_1 and δ_2 for the residuals, it is possible to detect all three faults f_1, f_2 and f_3 while minimising false alarms. Other scenarios have shown the difficulty in distinguishing fault cases f_1 and f_2 since these two faults have very similar effects on the system. Therefore, additional measurements may be needed to precisely identify which of the fault is occurring.

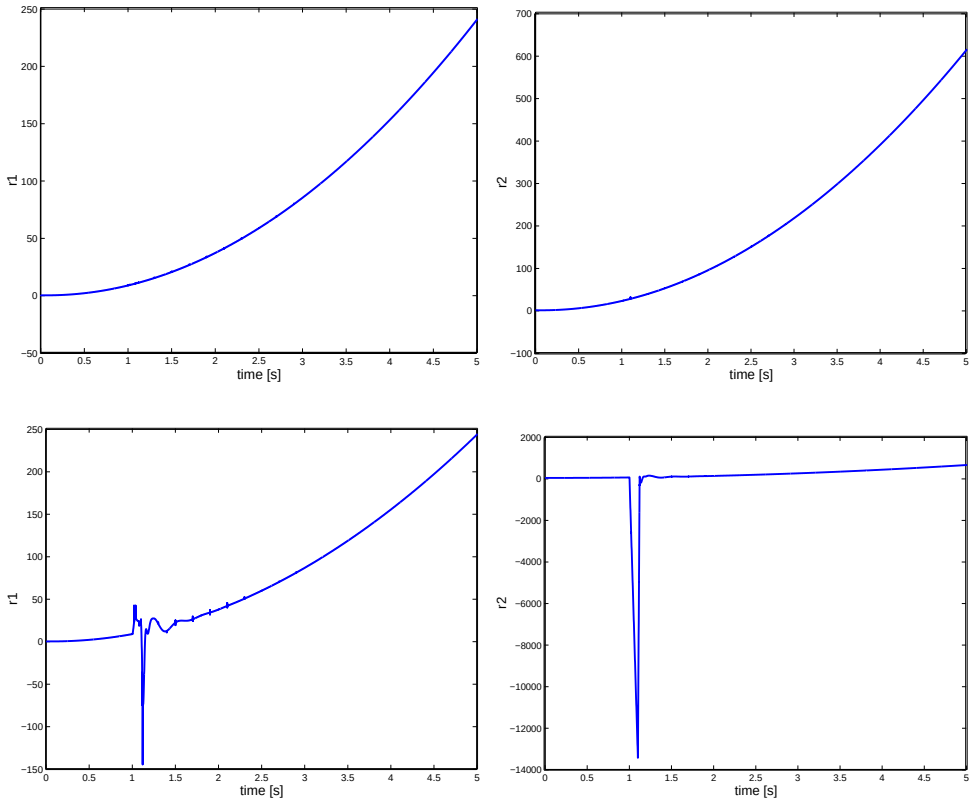

Figure 7: Residuals $R_1(t)$ and $R_2(t)$ generated from the simulation of fault-free (2 upper plots) and of fault case f_3 (2 lower plots). The fault occurs at $t = 1\,s$ and lasts less than $100\,ms$. By setting a threshold $\delta_1 = 100$ on residual $R_1(t)$ and $\delta_2 = 2000$ on $R_2(t)$ the fault is detected.

6 Conclusion

This paper has given a detailed model of a rolling mill uncoiler process. This model is extended, such that faulty behaviours can be simulated as well. This model is used to generate close-to-reality simu-

lations and to evaluate a model-based diagnostic method. Additionally a simplified model is derived, which is used to construct a diagnostic function based on residuals. In simulation, these residuals have shown to react sensitively to faulty behaviours.

Even with the strong assumptions used, experience shows that the fault detectability property is most likely to transpose to other diagnostic methods. Therefore, as a result of this research it can be said that, under ideal assumptions, model-based process diagnosis allows the detection of different faults occurring at the uncoiler.
Upcoming research includes dealing with practical operating conditions. This includes handling the time limited validity of the model, dealing with noisy measurements and developing robust algorithms with respect to intrinsic uncertainties in model parameters.
Models of the faulty behaviours may be included in the diagnosis to obtain fault *isolation*, *i.e.* to know *which* fault has occured in the system, instead of only knowing that *a* fault has occured (fault *detection*).

References

[1] G.F. Bryant. *Automation of tandem mills*. The Iron and Steel Institute, 1973.

[2] J.J. Gertler. *Fault Detection and Diagnosis in Engineering Systems*. Marcel Dekker, 1998.

[3] F. Holzweissig and H. Dresig. *Lehrbuch der Maschinendynamik*. Springer Verlag, 1982.

[4] J. Lunze, J. Chen, P.M. Frank, M. Kinnaert, and R.J. Patton. Fault Detection and Isolation. In: K. Åström *et al.* (Eds.) *Control of Complex Systems*, pages 191–207. Springer, 2001.

[5] R.J. Patton, P.M. Frank, and R.N. Clark. *Issues of Fault Diagnosis for Dynamic Systems*. Springer, 2000.

[6] M.M. Tiller. *Introduction to Physical Modeling with Modelica*. Kluwer Academic, 2001.